Applied Numerical Modeling in Geomechanics – 2016 – Gómez, Detournay, Hart & Nelson (eds.) Paper: 04-02

Plastic hardening model I: Implementation in *FLAC3D*

Z. Cheng & C. Detournay
Itasca Consulting Group, Inc., Minneapolis, MN, USA

ABSTRACT: The plastic hardening model with nonlinear volumetric and shear hardening capabilities, has been implemented in *FLAC3D* (Itasca 2012). A smooth cut-off technique that allows for possible contraction before the mobilized friction reaches the transformation angle is introduced to complement Rowe's dilation law. A semi-implicit iterative algorithm is developed as part of the model implementation. This algorithm is shown to be efficient and capable to handle accurately any elastic stress overshoots of the yield envelope. Verification examples are included to demonstrate the model capabilities and good functionality.

1 INTRODUCTION

The conventional Mohr-Coulomb (MC) model is widely used in civil engineering, and in particular for factor of safety predictions in slope engineering, using the strength reduction method. The MC model uses a constant modulus for both loading and unloading. If the modulus is taken as the initial slope from a stress-strain lab test curve, it will underestimate the deformation before failure; if the modulus is approximated as an averaged modulus measure before failure, the unloading-reloading modulus may not be appropriate, and could be responsible for unrealistic lift prediction behind a retaining wall after excavation. The plastic hardening (PH) model is based on the work by Schanz et al. (1999), who extended the hyperbolic Duncan-Chang non-linear elastic model (Duncan & Chang 1970) in an elasto-plastic framework to provide a more realistic pre-failure stress-strain behavior, and a more robust unloading/reloading scheme. The PH model is characterized by different modulus for primary loading and unloading/reloading. Also, the yield surface is not fixed in the principal stress space in the PH model; instead it can expand as a function of plastic strain; this yield surface behavior is referred to as plastic strain hardening. There are two types of hardening, namely shear hardening and volumetric (cap) hardening, in this model.

In this paper, we mainly present the implementation of the model with a semi-implicit algorithm into *FLAC3D*, and demonstrate some verification examples. The detail calibration for the material parameters and validation are presented in Cheng & Lucarelli (2016) and a design application is presented in Lucarelli & Cheng (2016). These two, together with this paper, consist of a series of papers on the PH model in the finite differential software platform.

In this document, all stresses are assumed to be effective stresses and are taken positive for extension. Principal stresses are labeled in the following order: $\sigma_1 \leq \sigma_2 \leq \sigma_3$.

2 FORMULATION

The PH model is based on the conventional elasto-plastic theory that assumes that the elastic and plastic strain increments are additive, i.e. $\Delta\varepsilon_{ij} = \Delta\varepsilon_{ij}^{e} + \Delta\varepsilon_{ij}^{p}$.

2.1 *Incremental Elastic Law*

The elastic behavior of the PH model is derived in the context of hypo-elasticity:

$$\Delta p = -K\Delta\varepsilon_v^e \tag{1.a}$$

$$\Delta s_{ij} = 2G\Delta\epsilon_{ij}^e \tag{1.b}$$

where p is the mean pressure defined as $p = -\sigma_{ii}/3$, ε_v^e is the volumetric elastic strain defined as $\varepsilon_v^e = \varepsilon_{ii}$, and s_{ij} and ϵ_{ij}^e are the deviatoric stress tensor and deviatoric elastic strain tensor, respectively. K and G are the elastic bulk and shear moduli, which can be derived from the elastic unloading-reloading Young's modulus, E_{ur}, and the elastic unloading-reloading Poisson's ratio, v, using the relations

$$K = \frac{E_{ur}}{3(1-2v)} \tag{2.a}$$

$$G = \frac{E_{ur}}{2(1+v)} \tag{2.b}$$

In the PH model, the Poisson's ratio is assumed to be constant with a typical value of 0.2 (if otherwise not provided at input), while the Young's modulus, and E_{ur} is a stress-dependent parameter:

$$E_{ur} = E_{ur}^{ref}\left(\frac{c\cdot\cot\phi-\sigma_3}{c\cdot\cot\phi+p^{ref}}\right)^m \tag{3}$$

where E_{ur}^{ref}, m, c, p^{ref} and ϕ are user-defined constant parameters. E_{ur}^{ref} is the reference unloading-reloading modulus at the reference pressure p^{ref}. The unloading-reloading modulus depends on the maximum (minimum compressive) principal stress σ_3, the cohesion c, and the ultimate friction angle ϕ, as well as the power m. For clays, m is usually close to 1. For sands, m is usually between 0.5 and 1.

The PH model also employs another modulus measure, E_{50}, which defines the shape of the primary shear hardening surface and obeys the following power law:

$$E_{50} = E_{50}^{ref}\left(\frac{c\cdot\cot\phi-\sigma_3}{c\cdot\cot\phi+p^{ref}}\right)^m \tag{4}$$

here E_{50}^{ref} is a material parameter, which could be estimated from multiple sets of triaxial compression tests with various cell stresses.

2.2 *Shear hardening*

The shear yield function is defined as

$$f_s = \left(\frac{q_a}{q_a-q} - \frac{E_i}{E_{ur}}\right)q - \frac{E_i}{2}\gamma^p = 0 \tag{5}$$

where $E_i = 2E_{50}/(2-R_f)$, E_i/E_{ur} is a constant (see Eq.(3) and (4)), $q = \sigma_3 - \sigma_1$, and q_a is given as

$$q_a = \frac{q_f}{R_f} = K_{qa}(c\cdot\cot\phi - \sigma_3) \tag{6}$$

where $K_{qa} = 2\sin\phi/((1-\sin\phi)R_f)$. The failure ratio R_f has a value smaller than 1, and R_f = 0.9 in most cases. The ultimate deviatoric stress $q_f = 2\sin\phi\,(c\cdot\cot\phi - \sigma_3)/(1-\sin\phi)$ is consistent with the MC failure law.

The shear hardening parameter γ^p is defined incrementally as

$$\Delta\gamma^p = -(\Delta\varepsilon_1^p - \Delta\varepsilon_2^p - \Delta\varepsilon_3^p) \tag{7}$$

Due to the increase of γ^p, the shear yield surface will expand, but the ultimate surface is still the conventional MC failure surface.

The PH model uses the following flow rule between plastic volumetric and shear strains:

$$\Delta\varepsilon_v^p = \sin\psi_m\ \Delta\gamma^p \tag{8}$$

where ψ_m is the mobilized dilation angle, which is smaller or equal to the user-defined ultimate dilation angle ψ. The mobilized dilation angle obeys the Rowe dilatancy law (1962):

$$\sin\psi_m = F_c \frac{\sin\phi_m - \sin\phi_{cv}}{1-\sin\phi_m \sin\phi_{cv}},\ if\ \sin\phi_m \le \sin\phi_{cv} \tag{9.a}$$

$$\sin\psi_m = \frac{\sin\phi_m - \sin\phi_{cv}}{1-\sin\phi_m \sin\phi_{cv}},\ if\ \sin\phi_m > \sin\phi_{cv} \tag{9.b}$$

Where the parameter F_c is the contraction scale factor, with an allowable range of 0 to 0.25. The critical state friction angle ϕ_{cv} is defined as

$$\sin\phi_{cv} = \frac{\sin\phi - \sin\psi}{1-\sin\phi \sin\psi} \tag{10}$$

The mobilized friction ϕ_m is defined in terms of the current stress state

$$\sin\phi_m = \frac{\sigma_1 - \sigma_3}{\sigma_1 + \sigma_3 - 2c\cdot\cot\phi} \tag{11}$$

A non-associated flow rule, consistent with a MC yield criterion is used in the model. The shear potential function is defined as

$$g_s = m_1\sigma_1 + m_3\sigma_3 \tag{12}$$

where $m_1 = (-1+\sin\psi_m)/2$, and $m_3 = (1+\sin\psi_m)/2$.

In order to avoid over-dilatancy when soil reaches its critical void state with e_{max}, the dilation angle needs a minor modification. One way proposed by Schanz et al. (1999) is to set a cut-off rule, so that

$$\sin\psi_m = 0, \qquad \text{if}\quad e \ge e_{max} \tag{13}$$

Here we introduce a smoothing technique to avoid sudden change of dilation angle:

$$\sin\psi_m = 100\left(1-\frac{e}{e_{max}}\right), \qquad \text{if}\quad e \ge 0.99e_{max} \tag{14}$$

The dilation rules with cut-off and the smoothing technique are compared with the case without dilation cut-off in Figure 1.

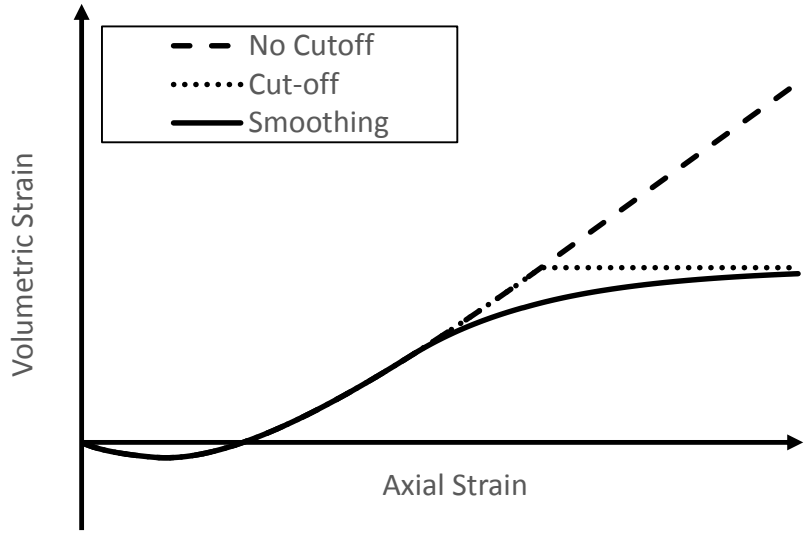

Figure 1. Volumetric strain curve for a standard triaxial compression test with dilation cut-off and smoothing.

2.3 *Volumetric hardening*

The volumetric (cap) yield function is defined as

$$f_v = g_v = \frac{\tilde{q}^2}{\alpha^2} + p^2 - p_c^2 = 0 \tag{15}$$

where α is a constant derived internally from other material parameters based on a virtual oedometer loading test; $\tilde{q}$ is a shear stress measure defined as $\tilde{q} = -[\sigma_1 + (\delta - 1)\sigma_2 - \delta\sigma_3]$, and $\delta = (1 + \sin\phi)/(1 - \sin\phi)$. The initial value of the hardening parameter p_c, which denotes the pre-consolidation pressure, can be determined using the initial stress state and an input material parameter *ocr*, so that

$$p_{c,ini} = ocr * \sqrt{\frac{\tilde{q}_{ini}^2}{\alpha^2} + p_{ini}^2} \tag{16}$$

If *ocr* assumes a large enough value, the model behaves as if the cap was non-existent.

The associated flow rule is adopted for volumetric hardening (i.e. the potential volumetric function has the same form as the volumetric yield function).

The volumetric hardening parameter γ^p is defined incrementally as

$$\Delta\gamma^p = -\Delta\varepsilon_v^p \tag{17}$$

where $\Delta\varepsilon_v^p$ is the plastic volumetric strain increment.

Evolution of the hardening parameter p_c is given by the relation:

$$\Delta p_c = H_p \Delta\gamma^v = H_c \left(\frac{c\cdot\cot\phi + p_c}{c\cdot\cot\phi + p^{ref}}\right)^m \Delta\gamma^v \tag{18}$$

where $H_p = H_c \left(\frac{c\cdot\cot\phi + p_c}{c\cdot\cot\phi + p^{ref}}\right)^m$, and H_c is a constant parameter derived internally from other material parameters according to a virtual oedometer test..

Instead of taking α and H_c as input material parameters, another two parameters, K_{nc} and E_{oed}^{ref} are specified as input. K_{nc} denotes normal consolidation coefficient and E_{oed}^{ref} stands for the tangent oedometer modulus at the reference pressure p^{ref}. If K_{nc} is not provided by the user, it is taken as $K_{nc} = 1 - sin\phi$ (default value).

2.4 *Tension failure*

The model will check for the tension failure condition. The tension failure and potential functions are

$$f_t = g_t = \sigma_3 - \sigma^t \tag{19}$$

where σ^t is the tension limit. By default, σ^t is zero and user can provide value up to the upper limit $\sigma_{lim}^t = c/\tan\phi$.

3 IMPLEMENTATION

In the implementation of the PH model, an elastic trial, σ_{ij}^I, is first computed after adding to the old stress components, σ_{ij}^o, increments calculated by application of Hooke's law to the total strain increment $\Delta\epsilon_{ij}$ for the step. During this step, the moduli and, mobilized dilation angle are assumed constant for simplicity based on the old stress components. All stresses are in terms of effective measurement.

The formulation for the trial stresses are:

$$\sigma_1^I = \sigma_1^o + E_1\Delta\varepsilon_1 + E_2(\Delta\varepsilon_2 + \Delta\varepsilon_3) \tag{20.a}$$

$$\sigma_2^I = \sigma_2^o + E_1\Delta\varepsilon_2 + E_2(\Delta\varepsilon_3 + \Delta\varepsilon_1) \tag{20.b}$$

$$\sigma_3^I = \sigma_3^o + E_1\Delta\varepsilon_3 + E_2(\Delta\varepsilon_1 + \Delta\varepsilon_2) \tag{20.c}$$

where $E_1 = K + 4G/3$, and $E_2 = K - 2G/3$, and $(\Delta\varepsilon_1, \Delta\varepsilon_2, \Delta\varepsilon_3)$ is the set of principal strain increments.

The trial internal variables, γ^p and $\gamma^v = -\varepsilon_v^p$ are assumed the same values from the last step. If the yield criteria is not satisfied, both the stress components and internal variables will be corrected.

3.1 *Shear hardening*

If $f_s > 0$, shear hardening will occur. The plastic strain increment is oriented in the direction of the gradient of the potential function in the principal stress space:

$$\Delta\varepsilon_1^p = \lambda_s \frac{\partial g_s}{\partial \sigma_1} = \lambda_s m_1 \tag{23.a}$$

$$\Delta\varepsilon_2^p = \lambda_s \frac{\partial g_s}{\partial \sigma_2} = 0 \tag{23.b}$$

$$\Delta\varepsilon_3^p = \lambda_s \frac{\partial g_s}{\partial \sigma_3} = \lambda_s m_3 \tag{23.c}$$

and

$$\Delta\gamma^p = -\left(\Delta\varepsilon_1^p - \Delta\varepsilon_2^p - \Delta\varepsilon_3^p\right) = \lambda_s \tag{24}$$

The corrected stress components are:

$$\sigma_1 = \sigma_1^I - \lambda_s(E_1 m_1 + E_2 m_3) \tag{25.a}$$

$$\sigma_2 = \sigma_2^I - \lambda_s(E_2 m_1 + E_2 m_3) \tag{25.b}$$

$$\sigma_3 = \sigma_3^I - \lambda_s(E_1 m_3 + E_2 m_1) \tag{25.c}$$

and the corrected interval variable is

$$\gamma^p = \gamma^{p,I} + \Delta\gamma^p = \gamma^{p,I} + \lambda_s \tag{26}$$

The derived shear stress is then

$$q = \sigma_3 - \sigma_1 = q^I - \lambda_s \cdot 2G \tag{27}$$

$$q_a = q_a^I + \lambda_s \cdot K_{qa}(E_1 m_3 + E_2 m_1) \tag{28}$$

Substitute the corrected q, q_a, γ^p into the shear function f_s, λ_s can then be solved from a nonlinear equation $f_s(\lambda_s) = 0$ either by a closed-form formulation or by an iteration method. Note that γ^p is using the current value related to the current λ_s, which implies that this correction algorithm uses a semi-implicit approach. If the trial stress is out of the shear failure surface (MC yield surface), the conventional MC model implementation applies.

3.2 *Volumetric hardening*

If $f_v > 0$, the volumetric hardening will occur. The plastic strain increment is related to the gradient of the potential function in stress space:

$$\Delta\varepsilon_1^p = \lambda_v \frac{\partial g_v}{\partial \sigma_1} = \lambda_v \left[-\frac{2\tilde{q}}{\alpha^2} - \frac{2}{3}p\right] \tag{29.a}$$

$$\Delta\varepsilon_2^p = \lambda_v \frac{\partial g_v}{\partial \sigma_2} = \lambda_v \left[-\frac{2\tilde{q}}{\alpha^2}(\delta - 1) - \frac{2}{3}p\right] \tag{29.b}$$

$$\Delta\varepsilon_3^p = \lambda_v \frac{\partial g_v}{\partial \sigma_3} = \lambda_v \left[\frac{2\tilde{q}}{\alpha^2}\delta - \frac{2}{3}p\right] \tag{29.c}$$

Evolution of the hardening parameter $\Delta\varepsilon_v^p$ is given by the relation:

$$\Delta\lambda^v = -\Delta\varepsilon_v^p = -(\Delta\varepsilon_1^p + \Delta\varepsilon_2^p + \Delta\varepsilon_3^p) = 2p\lambda_v \tag{30}$$

In the above formulation, the plastic strain and volumetric hardening parameter increment is related to the current stress measurement (p, or $\tilde{q}$), so the correction algorithm uses a semi-implicit approach.

The corrected stress components are

$$\sigma_1 = \sigma_1^I + \left[2pK + \frac{4\tilde{q}G}{\alpha^2}\right]\lambda_v \tag{31.a}$$

$$\sigma_2 = \sigma_2^I + \left[2pK + \frac{4(\delta-1)\tilde{q}G}{\alpha^2}\right]\lambda_v \tag{31.b}$$

$$\sigma_3 = \sigma_3^I + \left[2pK - \frac{4\delta\tilde{q}G}{\alpha^2}\right]\lambda_v \tag{31.c}$$

Noting that $p = -(\sigma_1 + \sigma_2 + \sigma_3)/3$, and $\tilde{q} = -[\sigma_1 + (\delta - 1)\sigma_2 - \delta\sigma_3]$, we get

$$p = \frac{p^I}{1+2K\lambda_v} \tag{32}$$

$$\tilde{q} = \frac{\tilde{q}^I}{1+2M\lambda_v} \tag{33}$$

where $M = 4G(\delta^2 - \delta + 1)/\alpha^2$. After substituting the corrected p and $\tilde{q}$ into the yield function f_v, λ_v is found by solving the nonlinear equation $f_v(\lambda_v) = 0$ for the smallest root using an iterative method.

3.3 *Combined shear/volumetric hardening*

It is possible that after the elastic trial, the stress is out of both the shear yield surface and volumetric yield surface. In this case, the plastic strain increment is related to the partial derivatives of the potential function as follows:

$$\Delta\varepsilon_1^p = \lambda_m \frac{\partial g_s}{\partial \sigma_1} + \lambda_v \frac{\partial g_v}{\partial \sigma_1} = \lambda_m m_1 + \lambda_v \left[-\frac{2\tilde{q}}{\alpha^2} - \frac{2}{3}p\right] \tag{34.a}$$

$$\Delta\varepsilon_2^p = \lambda_m \frac{\partial g_s}{\partial \sigma_2} + \lambda_v \frac{\partial g_v}{\partial \sigma_2} = \lambda_v \left[-\frac{2\tilde{q}}{\alpha^2}(\delta - 1) - \frac{2}{3}p\right] \tag{34.b}$$

$$\Delta\varepsilon_3^p = \lambda_m \frac{\partial g_s}{\partial \sigma_3} + \lambda_v \frac{\partial g_v}{\partial \sigma_3} = \lambda_m m_3 + \lambda_v \left[\frac{2\tilde{q}}{\alpha^2}\delta - \frac{2}{3}p\right] \tag{34.c}$$

λ_m and λ_v can be solved by an iterative method similar to that used in the shear or volumetric hardening correction technique. If the trial stress is out of both the volumetric hardening surface and MC failure surface, MC failure function should be used instead of the shear hardening function.

3.4 *Implementation procedure*

The implementation procedure is: in the initialization, the initial stress, evolution parameters and strain increment are defined for the zone and are assumed to be constant during this step. For simplicity, the moduli and dilation, which are dependent on the current stress and evolution parameters, are also assumed constants in the zone during this step. The trial elastic stresses and the possible stress corrections are defined at the sub-zone level. The trial stress increments obey the linear elastic (Hooke's) law. If the trial stresses violate the tension limit, the tension failure procedure is called. The next step is to check whether the tension-corrected stress is in the tension or compression side. If in the tensions side, volumetric hardening will not apply. In either side, if the stress is out of the shear failure or shear yield surface, the shear failure or hardening procedure will be called respectively. In the compression side, if the stress is out of the volumetric yield surface, the volumetric hardening procedure will be called. In particular, if the stress is also out of the shear failure or shear yield surface, the mixed procedure with both the volumetric hardening and shear failure/hardening procedure will be called. A second tension failure procedure is called if any volumetric hardening or shear hardening/failure occurs to ensure that the averaged stress in the zone-level is within the tension limit. After all sub-zones complete the stress check for tension and shear failure, shear and volumetric hardening criteria, the internal variables, moduli and dilation are then updated based on the zone average stresses.

4 VERIFICATION EXAMPLES

4.1 *Comparison with MC model*

This example compares the plastic hardening and Mohr-Coulomb model behavior. The constitutive models are used in a one-zone triaxial compression test with a constant cell pressure of 100 kPa. The strength parameters including friction angle, dilation angle, and tension limit are the

same for both models. The E_{50} modulus of the PH model is used as Young's modulus for the MC model and E_{ur} is assumed to be three times the value of E_{50}^{ref}. Figure 3 shows a plot of deviatoric stress versus axial strain for both PH and MC models. It is easy to verify from Figure 2 that: (1) The ultimate failure deviatoric stresses are the same for both models, as expected; (2) Looking at the pre-failure curve, the PH and MC models are crossing at half the value of the failure stress, which is consistent with the concept of E_{50} modulus; and (3) The unloading modulus in the MC model is the same as the loading modulus while these moduli are different in the PH model.

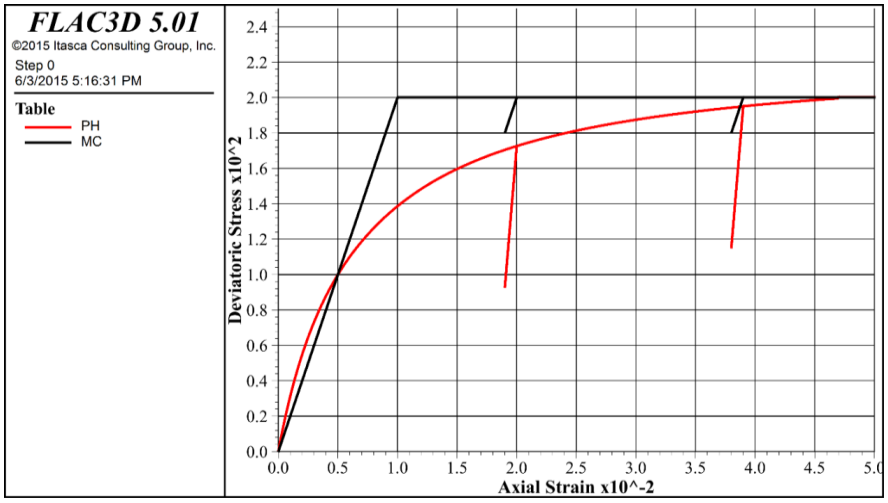

Figure 2. Comparison of PH and MC models for a triaxial compression test.

4.2 *Triaxial compression test*

Drained triaxial tests on dense, medium and loose sands are simulated using the PH model. The *ocr* is set to a large value in order to prevent yielding on the cap. A plot of deviatoric stress versus axial strain is shown in Figure 3. As expected, the plots show a hyperbolic behavior. The unloading-reloading paths are also shown in the figure. The plot of volumetric strain versus axial strain is shown in Figure 4. The dilatancy of the denser sands is clearly represented. The smooth decrease of the dilation angle when the void ratio is approaching the critical state occurs as a result of the dilation smoothing technique implemented in the model logic.

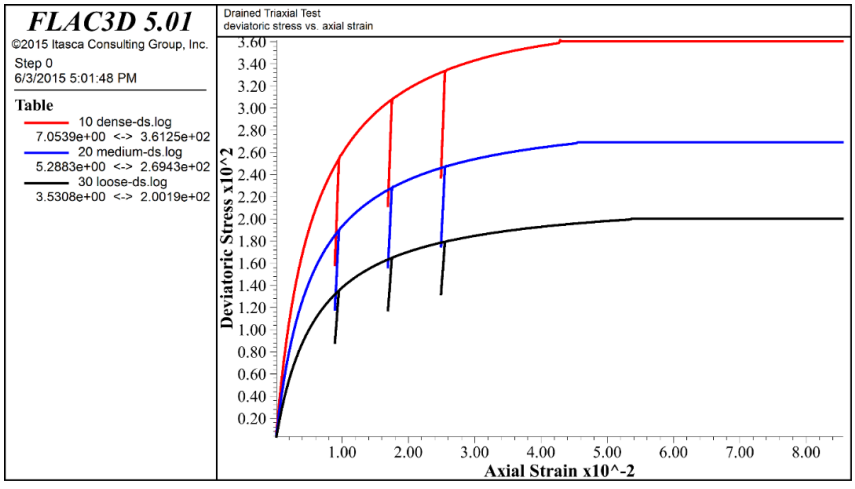

Figure 3. Drained triaxial deviatoric stress versus axial strain for dense, medium and loose sands.

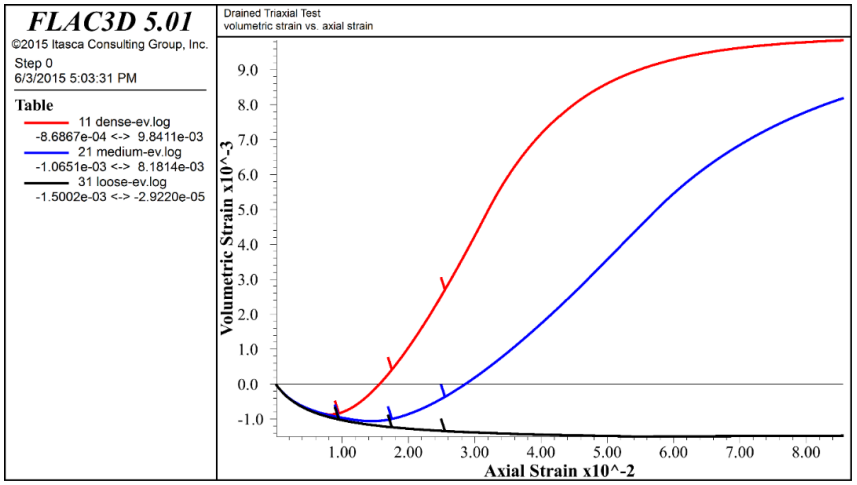

Figure 4. Volumetric strain versus axial strain for dense, medium and loose sands.

4.3 *Oedometer test*

This section presents the simulation of an oedometer test and shows the capability of the PH model to reproduce the evolution of lateral stress ratio $K_0 = \sigma_h/\sigma_v$. Three kinds of sand with friction angles of 30, 35, and 40 degrees are used in the simulations and the default consolidation coefficient is calculated as $K_{nc} = 1 - sin\phi$. Initially the model is in equilibrium with an isotropic stress state in each zone, $\sigma_{ii} = -0.1$ kPa. The results of stress ratio evolution due to compression in the oedometer test are shown in Figure 5, and it is seen that they correctly reproduce the expected evolution path. Figure 6 presents vertical oedometer pressure versus vertical strain, which reproduces the expected oedometer modulus at the reference vertical pressure of 100 kPa.

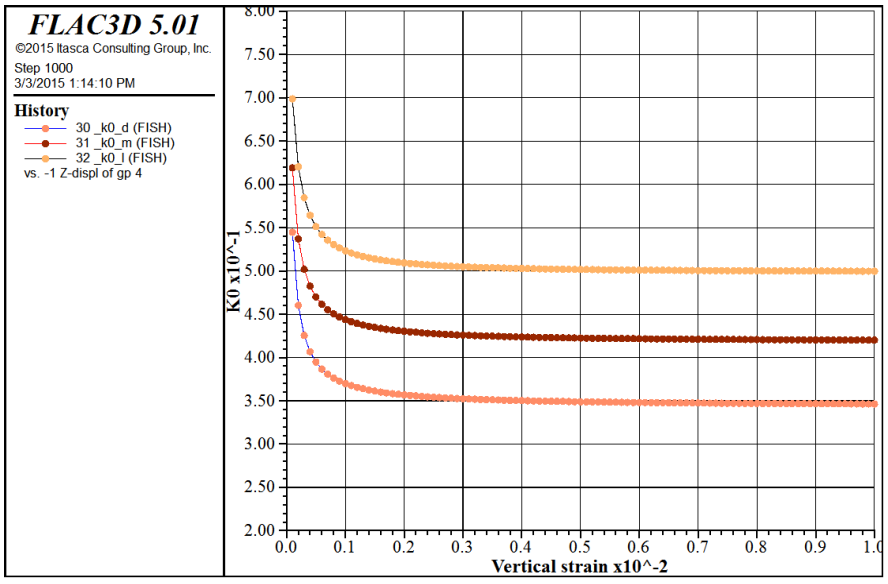

Figure 5. K_0 path calculated from the oedometer test with friction angles of 30, 35 and 40 degrees and default K_{nc} values.

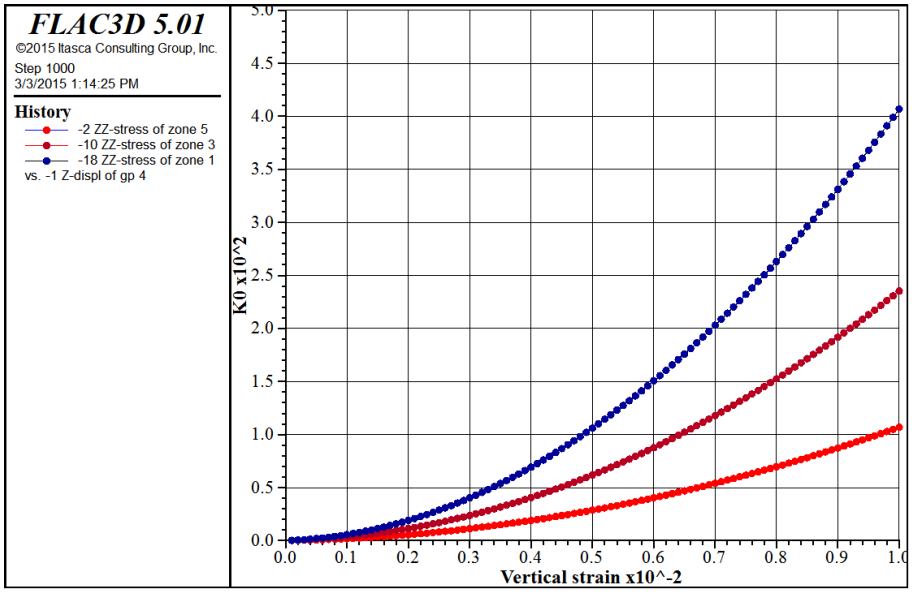

Figure 6. Vertical pressure versus vertical strain from the oedometer test with friction angles of 30, 35 and 40 degrees and default K_{nc} values.

4.4 *Load-step sensitivity test*

In the implementation of the PH model, we used a semi-implicit algorithm through iteration within the constitutive level as well as the least sensitivity of the load-steps. In order to test the loading step sensitivity, a one-zone isotropic compression test with a velocity-control approach but with very different load steps of 20,000, 2000, and 200 (so the controlling velocities are very different) are calculated (Fig. 7). It proves that, although the yield and hardening functions are nonlinear functions of the principal stresses, the implemented PH model correctly converges to the same result regardless of the very different load steps. However, it is not encouraged to use a very big load -step during a practice because the overall framework may request smaller load steps.

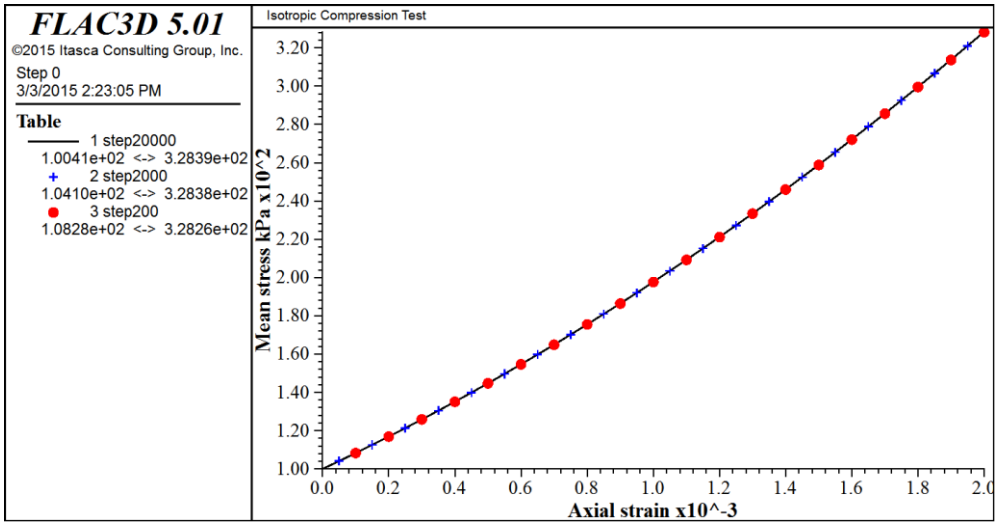

Figure 7. Load-step sensitivity testing with load steps = 20000, 2000, and 200.

5 SUMMARY

The new PH model formulated within the framework of hardening plasticity has been implemented into the platform of *FLAC3D* (Itasca 2012). The main features of the new PH model are: hyperbolic stress strain relationship in uniaxial drained compression; generation of plastic strain associated with mobilized friction (shear hardening); generation of plastic strain in primary compression (volumetric hardening); stress-dependent modulus according to a power law; elastic unloading/reloading compared to virgin loading; memory of pre-consolidation stress; and Mohr-Coulomb failure criterion. Verification examples show the model good performance. Calibration, validation, and application are not addressed here; they are included in companion papers (Cheng & Lucarelli 2016 and Lucarelli & Cheng 2016).

ACKNOWLEDGEMENT

Augusto Lucarelli, David DeGagné and Andrey Pyatigorets also contributed to the work either through the authors' discussion or to the editing of some sections of the paper. Their efforts are greatly acknowledged.

REFERENCES

Cheng, Z. & Lucarelli A. 2016. Plastic hardening model II: Calibration and validation. In P. Gomez, C. Detournay, R. Hart, M. Nelson (eds), Proc. 4th Itasca Symposium on Applied Numerical Modeling. March 7-9, 2016, Lima, Peru.

Duncan, J.M. & Chang, C.Y. 1970. Nonlinear analysis of stress and strain in soil. *J. Soil Mech. Found. Div.* 96(5), pp.1629-1653.

Itasca Consulting Group, Inc. 2012. *FLAC3D – Fast Lagrangian Analysis of Continua in 3 Dimensions, Ver. 5.0*. Minneapolis: Itasca.

Lucarelli, A & Cheng, Z. 2016. Plastic hardening model III: Design application. In P. Gomez, C. Detournay, R. Hart, M. Nelson (eds), Proc. 4th Itasca Symposium on Applied Numerical Modeling. March 7-9, 2016, Lima, Peru.

Rowe, P.W. 1962. The stress-dilatancy relation for static equilibrium of an assembly of particles in contact. *Proc. Roy. Soc. A.* 269(1339), pp.500-527.

Schanz, T., Vermeer, P.A. & Bonnier, P.G. 1999. The hardening soil model: formulation and verification. In R.B.J. Brinkgreve (ed), *Beyond 2000 in Computational Geotechnics -10 Years of Plaxis*. Rotterdam: Balkema.